Optical Thomson Scatter from a Mg Laser Ablated Plume

D Riley, A Delserieys, FY Khattak, E Nedanovska and CLS Lewis

School of Mathematics and Physics, Queen's University Belfast, Belfast, BT7 1NN, UK

Abstract

Optical Thomson scatter has been implemented as a diagnostic of laser ablated plumes under conditions relevant to pulsed laser deposition. The plumes have been generated with both KrF and second harmonic Nd:Yag laser radiation. Thomson scatter data with both spatial and temporal resolution has been collected giving both electron density and temperature.

Introduction

Laser ablated plumes created with nanosecond lasers operating at fluences of a few J/cm^2 are of great relevance to pulsed laser deposition of new technological materials [e.g. 1]. There has naturally been a great interest in understanding the dynamics of such plumes. To this end several diagnostic techniques, such as Laser induced fluorescence, interferometry, plasma imaging and particle probes have been employed.

Recently, we have added to this list by employing Thomson scatter [2,3]. This is a powerful technique that has been widely used in fusion plasmas as well as high temperature laser-plasmas and electrically driven RF plasmas. It has however, until now, not been used extensively in low temperature plumes of the sort investigated here. We have used both KrF (248nm) and second harmonic Nd:Yag (532nm) lasers and present some data from both in this paper.

Experimental set-up

The basic set up is shown in figure 1. To create the plasma plume, initially a KrF laser with 20ns Full width at half maximum (FWHM) duration was focused using a random phase plate to create a 1mm square focal spot. The fluence on target was 10J/cm^2. The target was a rotating disk of solid Mg that presented a new surface to each laser shot. The laser was operated at 10Hz and for each data point approximately 500 shots were integrated. The probe beam was a second harmonic Nd:Yag laser at 532nm, which was electronically synchronized to the ablation beam to about 10ns accuracy. The probe was loosely focused with ~f/200 optics to form a focal spot of ~0.5mm. The scattered light was collected at 90° and imaged onto a double grating spectrometer with two 1200l/mm gratings giving 5.7Å/mm dispersion.

The scatter spectrum was spatially resolved along a line parallel to the target surface. The spectrum was recorded with an intensified CCD camera with a 10ns gate that reduced the level of self-emission recorded from the plasma. By moving the target with respect to the incident ablating beam, the plume was probed from 2-5mm from the target surface at times from 100-1000ns after ablation. In a second series of experiments a second harmonic Nd:Yag was also used as an ablating pulse. In that case the focal spot was 0.8mm and the fluence used was varied from 10-30J/cm^2. The gated CCD prevented the ablating pulse from affecting the scatter probe results. In both cases the probe energy was chosen to be 50mJ as this was determined in preliminary shots to lead to insignificant probe heating of the plume. The gating of the CCD allowed the scattered probe signal to be separated from the scatter from the ablating beam easily. In figure 2 we show examples of the scatter spectrum recorded for scatter with 532nm. We see two cases, one at high and one at low scatter parameter α. This parameter is defined by, $\alpha = 1/k\lambda_D$ where k is the scatter wave-vector and λ_D is the Debye length. Its significance is that, at $\alpha >\sim 1$ we probe the collective oscillations of the electrons- hence the plasmon features in fig 2a, and at $\alpha << 1$ we probe the random thermal motions of the electrons and the scatter spectrum represents Doppler shifted scatter from the Maxwellian electron distribution. The sharp features either side of the Rayleigh line in the high α case are atomic Raman satellites originating from the meta-stable ^{3}P Mg level. These were seen in earlier data with KrF ablation and have been discussed elsewhere [4].

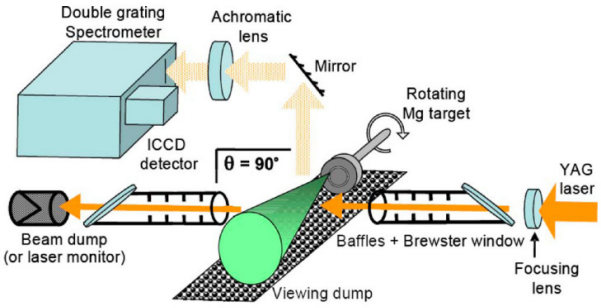

Figure 1. Schematic of experimental set up.

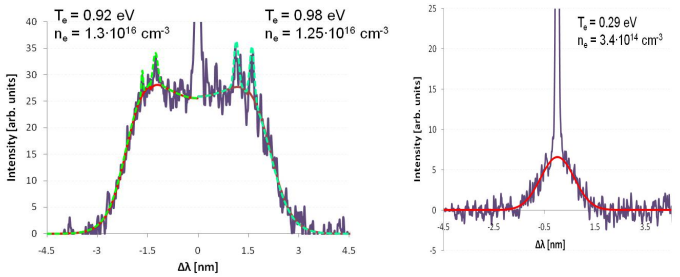

Figure 2 *above left*. Spectrum taken at 300ns after ablation, 2mm from the target with 30J/cm^2 fluence. *Above right*: Scatter at 2mm from target with15J/cm^2 fluence at 500ns after ablation. In both cases the ablating laser was at 532nm wavelength.

In figure 3 we can see a time history of the electron density and temperature for the case of 15J/cm^2 and 532nm and 2mm from target. For comparison, in figure 4 we see data for

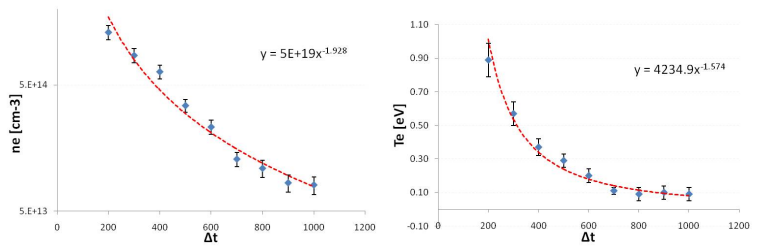

Figure 3. Electron density and temperature evolution for 2mm from target surface with 532nm irradiation at 15J/cm^2

ablation with 10J/cm^2 at 248nm. We notice that, in the KrF ablation case, the electron density falls off approximately as ~t^{-5} compared to ~t^{-3} for the Rayleigh signal. The latter is expected from simple 3D self-similar expansion, but the rapid fall in electron density is believed to be due to dielectronic recombination. For the peak electron density of ~10^{17} cm^{-3} and electron temperature of ~3eV the recombination time is ~230ns, [5] which is consistent with the fall off seen. Other recombination rates, such as radiative and three-body occur over micro-second scales for these conditions [6]. This case was also discussed elsewhere [3]. However, for the new data at 532nm, we see that the rate of fall for the electron density is much slower, in fact, close to the geometrically expected t^{-3} fall off. This indicates a much slower recombination. Analysis of the expected recombination rates indicates that this is expected. The electron density is lower as is the temperature and the radiative recombination timescale is several microseconds at early time.

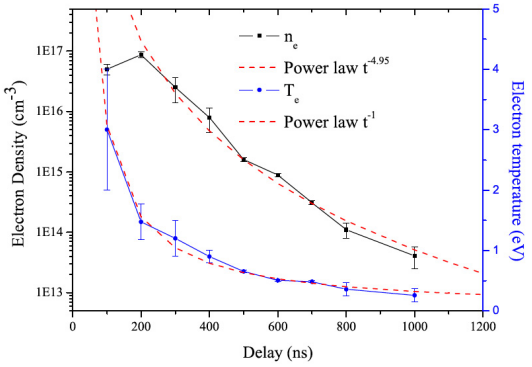

Figure 4. Electron density and temperature evolution for 2mm from target surface with 248nm irradiation at 10J/cm^2

Comparison of the data for 532nm ablation has been made with an analytical expansion model that assumes the plasma starts as a uniform slab and expands in three dimensions either isentropically or isothermally [7]. The results depend on several parameters that must be decided upon. There are a) axial and lateral expansion velocities b) ionization degree, since the model calculates atomic/ionic density and the scatter determines electron density c) mass in each ablated plume. For a) we have measured the lateral expansion from observing the extent of the scatter signal in the spatially resolved data, and found it to be ~1.0x10^6 cm/s at the plasma edge. Analysis of the density for different distances from target surface indicate that the ratio of axial to lateral expansion velocity to be ~2, which is typical for this spot size. The ablated mass was measured by firing 500 shots onto a single spot and measuring the crater left. This indicated that the upper limit per shot is 8x10^{-8} g. This may be an upper limit as some mass may be lost long after the initial ablation event as heat conduction allows a

slowly evaporating molten pool to be created beneath the initially ablated layer. This measured ablated mass is in fact more than 20 times smaller than would be expected from a simple model [8]. This is thought to be a result of screening of the target surface by the plasma formation [9lunney]. For the ionization, we used a collisional radiative model [10] to calculate that Z* at 200ns and 2mm from the target surface was 0.94. Comparing isothermal and isentropic models, we see in figure 5, that an isothermal model fits moderately well if we take the ablated mass to be $8x10^{-8}$g. An isentropic model fits only if the ablated mass is reduced by a further factor of ~25, well below the measured value. This indicates that, as with the KrF ablation case, an isothermal model of the plume fits better than an isentropic.

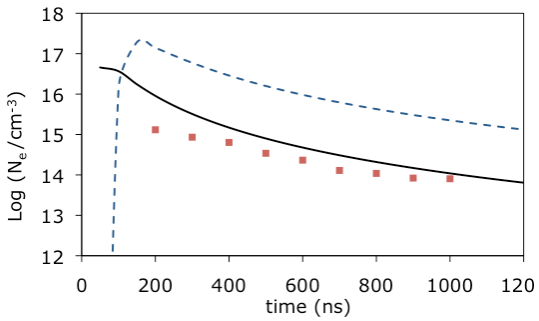

Figure 5 The squares are density data for 2mm from target at 200ns delay. The solid line is for an isothermal model of expansion and the dashed line for an isentropic model.

1. D. B. Chrisey and G. K. Hubler, Pulsed Laser Deposition of Thin Films, Wiley, New York, 2003 .
2. A Delserieys, FY Khattak, CLS Lewis and D Riley, Journal of Applied Physics, **106**, 083304, 2009
3. A Delserieys, FY Khattak, J. Pedregosa Gutierrez, CLS Lewis and D Riley, Appl. Phys. Lett. **92** 011502, 2008
4. A Delserieys, FY Khattak, S Sahoo, G Gribakin, CLS Lewis and D Riley, Phys. Rev. A **78** (5) 055404, 2008
5. A. Thum-Jaeger et al., Phys. Rev. E **61**, 3063 2000 .
6. Z. Altun, A. Yumak, N. R. Badnell, S. D. Loch, and M. S. Pindzola, Astron. Astrophys. **447**, 1165 2006.
7. M. W. Stapleton, A. P. McKiernan, and J.-P. Mosnier, J. Appl. Phys. **97**, 064904 2005 .
8. S. Amoruso, R. Bruzzese, R. Velotta, and N. Spinelli, J. Phys. B **32**, R131 1999
9. J. G. Lunney, Appl. Surf. Sci. 86, **79** 1995
10. D Riley *et al* Plasma Sources Sci. Technol. **9**(3) 270-278 (2000)